Probing Neutrino Transition Magnetic Moments at CEνNS Experiments

Dimitrios K. Papoulias

IFIC (CSIC-Valencia U.)

Erice School 2019, Sicily: September 16–24, 2019

Outline

Physics Motivations of CEνNS

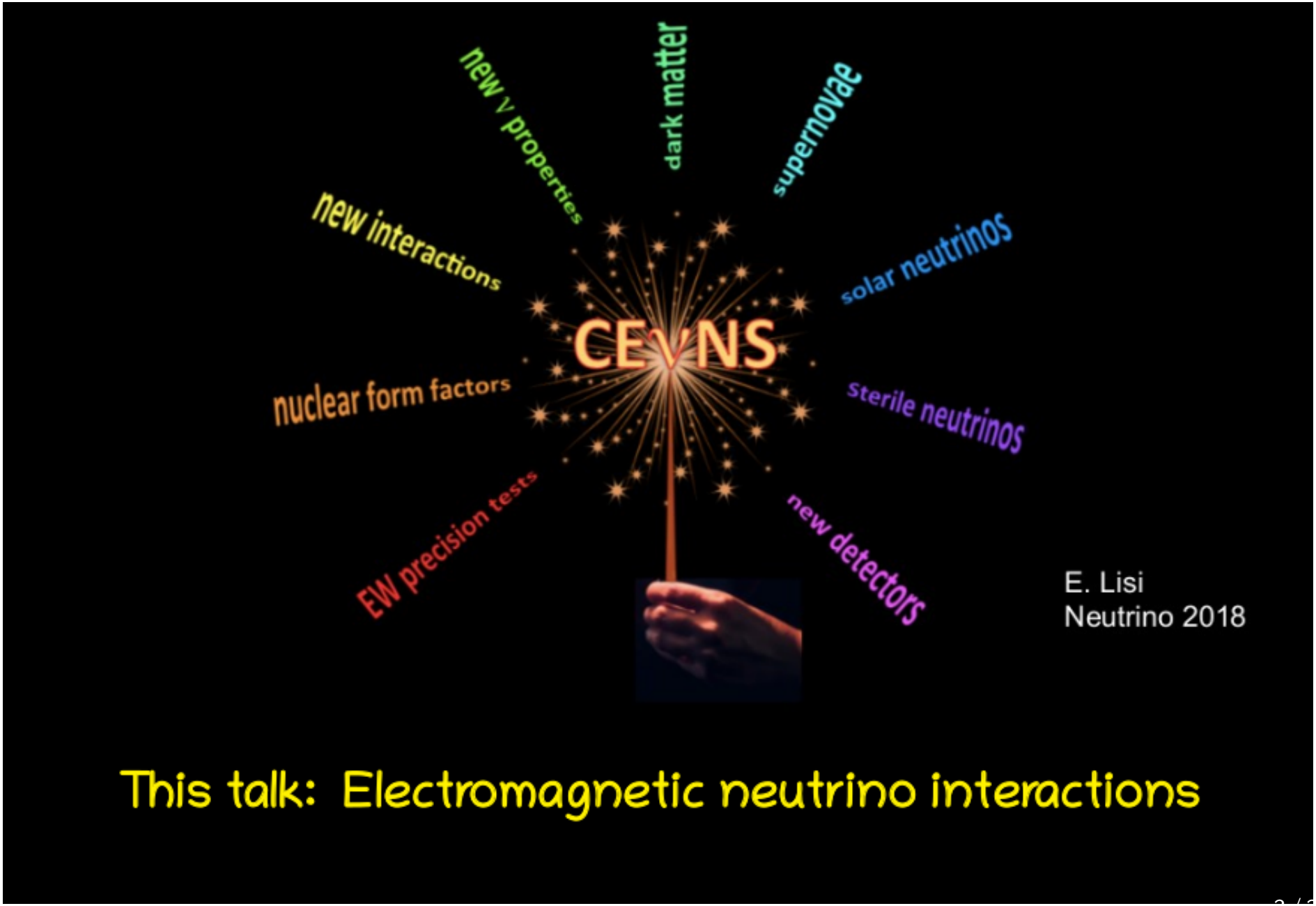

CEνNS experiments worldwide

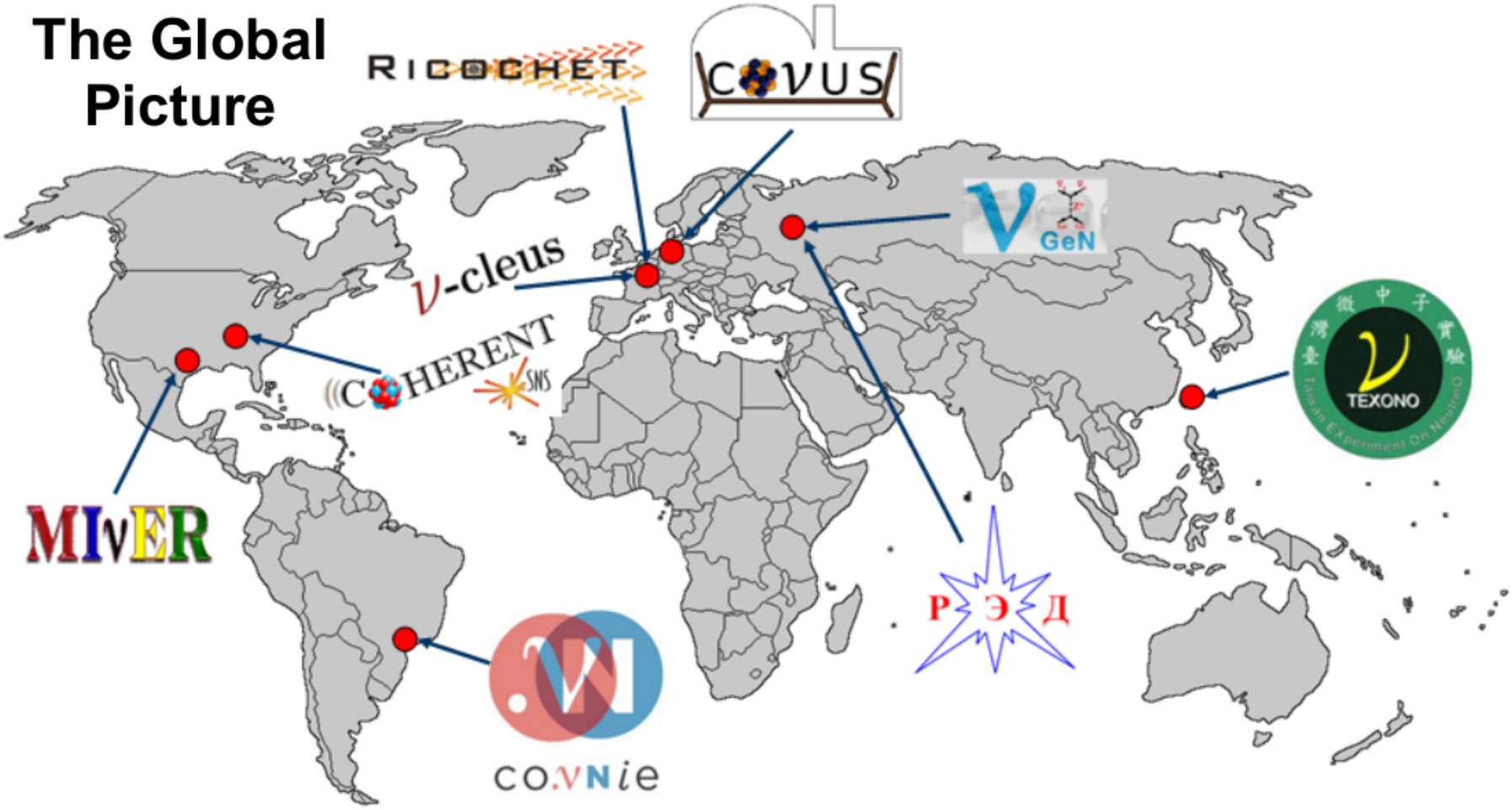

from M. Green: Aspen 2019 Winter Conference, March 2019

Science REPORTS

Cite as: D. Akimov *et al.*, *Science* 10.1126/science.aao0990 (2017).

Observation of coherent elastic neutrino-nucleus scattering

D. Akimov,[1,2] J. B. Albert,[3] P. An,[4] C. Awe,[4,5] P. S. Barbeau,[4,5] B. Becker,[6] V. Belov,[1,2] A. Brown,[4,7] A. Bolozdynya,[2] B. Cabrera-Palmer,[8] M. Cervantes,[5] J. I. Collar,[9]* R. J. Cooper,[10] R. L. Cooper,[11,12] C. Cuesta,[13]† D. J. Dean,[14] J. A. Detwiler,[13] A. Eberhardt,[13] Y. Efremenko,[6,14] S. R. Elliott,[12] E. M. Erkela,[13] L. Fabris,[14] M. Febbraro,[14] N. E. Fields,[9]‡ W. Fox,[3] Z. Fu,[13] A. Galindo-Uribarri,[14] M. P. Green,[4,14,15] M. Hai,[9]§ M. R. Heath,[3] S. Hedges,[4,5] D. Hornback,[14] T. W. Hossbach,[16] E. B. Iverson,[14] L. J. Kaufman,[3]‖ S. Ki,[4,5] S. R. Klein,[10] A. Khromov,[2] A. Konovalov,[1,2,17] M. Kremer,[4] A. Kumpan,[2] C. Leadbetter,[4] L. Li,[4,5] W. Lu,[14] K. Mann,[4,15] D. M. Markoff,[4,7] K. Miller,[4,5] H. Moreno,[11] P. E. Mueller,[14] J. Newby,[14] J. L. Orrell,[16] C. T. Overman,[16] D. S. Parno,[13]¶ S. Penttila,[14] G. Perumpilly,[9] H. Ray,[18] J. Raybern,[5] D. Reyna,[8] G. C. Rich,[4,14,19] D. Rimal,[18] D. Rudik,[1,2] K. Scholberg,[5] B. J. Scholz,[9] G. Sinev,[5] W. M. Snow,[3] V. Sosnovtsev,[2] A. Shakirov,[2] S. Suchyta,[10] B. Suh,[4,5,14] R. Tayloe,[3] R. T. Thornton,[3] I. Tolstukhin,[3] J. Vanderwerp,[3] R. L. Varner,[14] C. J. Virtue,[20] Z. Wan,[4] J. Yoo,[21] C.-H. Yu,[14] A. Zawada,[4] J. Zettlemoyer,[3] A. M. Zderic,[13] COHERENT Collaboration#

134 ± 22 events were measured at a 6.7-σ confidence level, using a low-background, 14.6-kg CsI[Na] scintillator within 308.1 live days

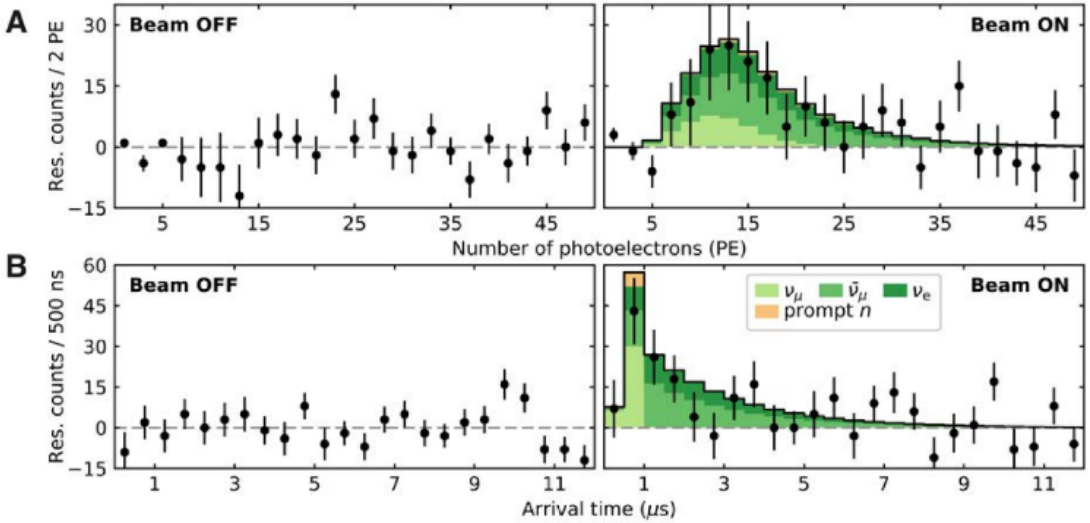

Members of the COHERENT team work with the world's smallest neutrino detector, the only one that can be lifted without heavy machinery. COHERENT COLLABORATION; PHOTOGRAPHER JUAN COLLAR

Milk jug–sized detector captures neutrinos in a whole new way

[COHERENT Collab. (Akimov et al.), Science **357** (2017) 1123]

Standard Model CEνNS cross section

CEνNS cross section expressed through the nuclear recoil energy T_A

$$\left(\frac{d\sigma}{dT_A}\right)_{\rm SM} = \frac{G_F^2 m_A}{\pi}\left[\mathcal{Q}_V^2\left(1-\frac{m_A T_A}{2E_\nu^2}\right)+\mathcal{Q}_A^2\left(1+\frac{m_A T_A}{2E_\nu^2}\right)\right]F^2(Q^2)$$

[DKP, Kosmas: PRD 97 (2018)]

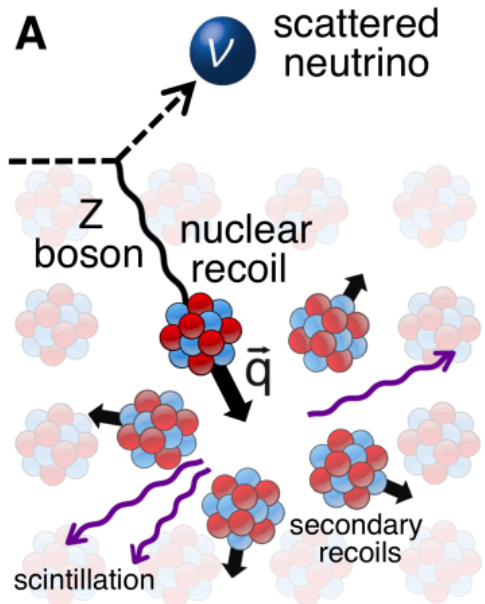

- E_ν: is the incident neutrino energy
- m_A: the nuclear mass of the detector material
- Z protons and $N = A - Z$ neutrons
- vector $\mathcal{Q}_V$ and axial vector $\mathcal{Q}_A$ contributions
- $F(Q^2)$: is the nuclear form factor

$$\mathcal{Q}_V = \left[2(g_u^L+g_u^R)+(g_d^L+g_d^R)\right]Z+\left[(g_u^L+g_u^R)+2(g_d^L+g_d^R)\right]N,$$
$$\mathcal{Q}_A = \left[2(g_u^L-g_u^R)+(g_d^L-g_d^R)\right](\delta Z)+\left[(g_u^L-g_u^R)+2(g_d^L-g_d^R)\right](\delta N),$$

- $(\delta Z) = Z_+ - Z_-$ and $(\delta N) = N_+ - N_-$, where Z_+ (N_+) and Z_- (N_-) refers to total number of protons (neutrons) with spin up or down [Barranco et al.: JHEP 0512 (2005)]

Electromagnetic contribution to CEνNS cross section

The Electromagnetic CEνNS cross section reads [Vogel, Engel.: PRD 39 [1989] 3378

$$\left(\frac{d\sigma}{dT_A}\right)_{\rm EM} = \frac{\pi a_{\rm EM}^2 \mu_\nu^2 Z^2}{m_e^2}\left(\frac{1-T_A/E_\nu}{T_A}\right) F^2(Q^2)\,.$$

- can be dominant for sub-keV threshold experiments
- may lead to detectable distortions of the recoil spectrum

The helicity preserving SM cross section adds incoherently with the helicity-violating EM cross section

$$\left(\frac{d\sigma}{dT_A}\right)_{\rm tot} = \left(\frac{d\sigma}{dT_A}\right)_{\rm SM} + \left(\frac{d\sigma}{dT_A}\right)_{\rm EM}$$

μ_ν^2 is the effective neutrino magnetic moment in the mass basis relevant to a given neutrino beam (reactor, SNS, etc.)

- Experimental measurements usually constrain some process-dependent effective parameter combination
- needs to be expressed in terms of fundamental parameters (TMMs + CP phases + mixing-angles)
- Even in the case of laboratory neutrino experiments, where the initial neutrino flux is fixed to have a well determined given flavor, there is no sensitivity to the final neutrino state

Electromagnetic neutrino vertex (spin component)

Dirac neutrinos: $H^{\mathrm{D}}_{\mathrm{EM}} = \frac{1}{2}\bar{\nu}_R \lambda \sigma^{\alpha\beta} \nu_L F_{\alpha\beta} + \mathrm{h.c.}$

- $\lambda = \mu - i\epsilon$ is an arbitrary complex matrix
- $\mu = \mu^\dagger$ and $\epsilon = \epsilon^\dagger$.

Majorana neutrinos: $H^{\mathrm{M}}_{\mathrm{EM}} = -\frac{1}{4}\nu_L^{\mathsf{T}} C^{-1} \lambda \sigma^{\alpha\beta} \nu_L F_{\alpha\beta} + \mathrm{h.c.}$

- $\lambda = \mu - i\epsilon$: antisymmetric complex matrix ($\lambda_{\alpha\beta} = -\lambda_{\beta\alpha}$)
- $\mu^{\mathsf{T}} = -\mu$ and $\epsilon^{\mathsf{T}} = -\epsilon$ are two imaginary matrices.
- three complex or six real parameters are required

In contrast to the Dirac case, vanishing diagonal moments are implied for Majorana neutrinos, $\mu^{\mathrm{M}}_{ii} = \epsilon^{\mathrm{M}}_{ii} = 0$.

[Schechter, Valle: PRD 24 (1981), PRD 25 (1982)]

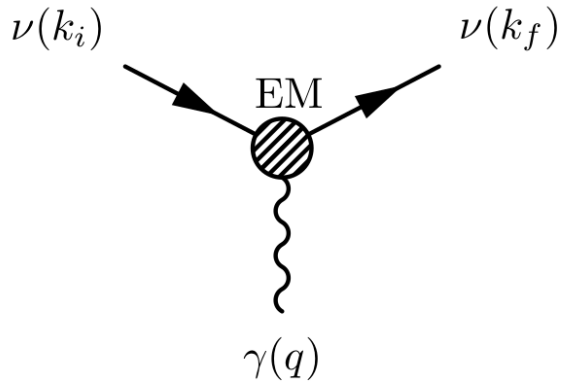

The neutrino transition magnetic moment (TMM) matrix

The magnetic moment matrix λ ($\tilde{\lambda}$) in the flavor (mass) basis reads

[Tórtola: PoS AHEP 2003 (2003)]

$$\lambda = \begin{pmatrix} 0 & \Lambda_\tau & -\Lambda_\mu \\ -\Lambda_\tau & 0 & \Lambda_e \\ \Lambda_\mu & -\Lambda_e & 0 \end{pmatrix}, \qquad \tilde{\lambda} = \begin{pmatrix} 0 & \Lambda_3 & -\Lambda_2 \\ -\Lambda_3 & 0 & \Lambda_1 \\ \Lambda_2 & -\Lambda_1 & 0 \end{pmatrix}$$

- the definition $\lambda_{\alpha\beta} = \varepsilon_{\alpha\beta\gamma}\Lambda_\gamma$ has been introduced,
- the neutrino TMMs are represented by the complex parameters

$$\Lambda_\alpha = |\Lambda_\alpha| e^{i\zeta_\alpha}, \qquad \Lambda_i = |\Lambda_i| e^{i\zeta_i}$$

three complex or six real parameters (3 moduli + 3 phases)

Effective neutrino magnetic moment @ experiments

Is expressed in terms of the neutrino magnetic moment matrix and the amplitudes of positive and negative helicity states 3−vectors $\mathfrak{a}_+$ and $\mathfrak{a}_-$,

- In the flavor basis one finds [Grimus, Schwetz: Nucl. Phys. B587 (2000)]

$$\left(\mu_\nu^F\right)^2 = \mathfrak{a}_-^\dagger \lambda^\dagger \lambda \mathfrak{a}_- + \mathfrak{a}_+^\dagger \lambda \lambda^\dagger \mathfrak{a}_+ \,,$$

Introducing the transformations (U is the lepton mixing matrix)

$$\tilde{\mathfrak{a}}_- = U^\dagger \mathfrak{a}_-, \qquad \tilde{\mathfrak{a}}_+ = U^\mathsf{T} \mathfrak{a}_+, \qquad \tilde{\lambda} = U^\mathsf{T} \lambda U \,,$$

- In the mass basis reads

$$\left(\mu_\nu^M\right)^2 = \tilde{\mathfrak{a}}_-^\dagger \tilde{\lambda}^\dagger \tilde{\lambda} \tilde{\mathfrak{a}}_- + \tilde{\mathfrak{a}}_+^\dagger \tilde{\lambda} \tilde{\lambda}^\dagger \tilde{\mathfrak{a}}_+$$

TMMs in flavor & mass basis @ reactor facilities

Reactor antineutrinos: $\bar{\nu}_e$ (where $\alpha_+^1 = 1$)

- flavor basis

$$\left(\mu^F_{\bar{\nu}_e,\,\text{reactor}}\right)^2 = |\Lambda_\mu|^2 + |\Lambda_\tau|^2$$

where $|\Lambda_\mu|$ and $|\Lambda_\tau|$ are the elements of the neutrino TMM matrix λ describing the corresponding conversions from the electron antineutrino to the muon and tau neutrino states

- mass basis [Cañas et al.: PLB 753 (2016)]

$$\begin{aligned}\left(\mu^M_{\bar{\nu}_e,\,\text{reactor}}\right)^2 =& |\boldsymbol{\Lambda}|^2 - c_{12}^2 c_{13}^2 |\Lambda_1|^2 - s_{12}^2 c_{13}^2 |\Lambda_2|^2 - s_{13}^2 |\Lambda_3|^2 \\ & - c_{13}^2 \sin 2\theta_{12} |\Lambda_1||\Lambda_2| \cos\xi_3 \\ & - c_{12} \sin 2\theta_{13} |\Lambda_1||\Lambda_3| \cos(\delta_{\text{CP}} - \xi_2) \\ & - s_{12} \sin 2\theta_{13} |\Lambda_2||\Lambda_3| \cos(\delta_{\text{CP}} - \xi_1)\,,\end{aligned}$$

with $|\boldsymbol{\Lambda}|^2 = |\Lambda_1|^2 + |\Lambda_2|^2 + |\Lambda_3|^2$ and

phase redefinition: $\xi_1 = \zeta_3 - \zeta_2$, $\xi_2 = \zeta_3 - \zeta_1$ and $\xi_3 = \zeta_1 - \zeta_2$

TMMs in flavor & mass basis @ SNS facilities (prompt)

Prompt beam: ν_μ (with $\alpha_-^2 = 1$)

- flavor basis

$$\left(\mu^F_{\nu_\mu,\,\text{prompt}}\right)^2 = |\Lambda_e|^2 + |\Lambda_\tau|^2$$

- mass basis

$$\begin{aligned}
\left(\mu^M_{\nu_\mu,\,\text{prompt}}\right)^2 = {} & |\Lambda_1|^2 \left[-2c_{12}c_{23}s_{12}s_{13}s_{23}\cos\delta_{\text{CP}}\right. \\
& \left. + s_{23}^2\left(c_{13}^2 + s_{12}^2 s_{13}^2\right) + c_{12}^2 c_{23}^2\right] \\
& + |\Lambda_2|^2 \left[2c_{12}c_{23}s_{13}s_{23}s_{12}\cos\delta_{\text{CP}} + c_{23}^2 s_{12}^2 + s_{23}^2\left(c_{12}^2 s_{13}^2 + c_{13}^2\right)\right] \\
& + |\Lambda_3|^2 \left[c_{23}^2 + s_{13}^2 s_{23}^2\right] \\
& + 2\,|\Lambda_1\Lambda_2| \left[c_{23}c_{12}^2 s_{13}s_{23}\cos\left(\delta_{\text{CP}} + \xi_3\right) - c_{23}s_{12}^2 s_{13}s_{23}\cos\left(\delta_{\text{CP}} - \xi_3\right)\right. \\
& \left. + c_{12}s_{12}\left(c_{23}^2 - s_{13}^2 s_{23}^2\right)\cos\xi_3\right] \\
& + 2\,|\Lambda_1\Lambda_3| \left[c_{13}s_{23}\left(c_{12}s_{13}s_{23}\cos\left(\delta_{\text{CP}} - \xi_2\right) + c_{23}s_{12}\cos\xi_2\right)\right] \\
& + 2\,|\Lambda_2\Lambda_3| \left[c_{13}s_{23}\left(s_{12}s_{13}s_{23}\cos\left(\delta_{\text{CP}} - \xi_1\right) - c_{12}c_{23}\cos\xi_1\right)\right] .
\end{aligned}$$

Miranda, DKP, Tórtola, Valle, JHEP 1907 (2019) 103

TMMs in flavor & mass basis @ SNS facilities (delayed ν_e)

Delayed beam: (i) ν_e (with $\mathfrak{a}_-^1 = 1$) and (ii) $\bar{\nu}_\mu$ (with $\mathfrak{a}_+^2 = 1$)

Focus on the ν_e component

- flavor basis

$$\left(\mu^F_{\nu_e,\,\text{delayed}}\right)^2 = |\Lambda_\mu|^2 + |\Lambda_\tau|^2$$

- mass basis

$$\begin{aligned}\left(\mu^M_{\nu_e,\,\text{delayed}}\right)^2 = {} & |\Lambda_1|^2\left[c_{13}^2 s_{12}^2 + s_{13}^2\right] + |\Lambda_2|^2\left[c_{12}^2 c_{13}^2 + s_{13}^2\right] + |\Lambda_3|^2\, c_{13}^2 \\ & - |\Lambda_1\Lambda_2|\left[c_{13}^2 \sin(2\theta_{12})\cos\xi_3\right] - |\Lambda_1\Lambda_3|\left[c_{12}\sin(2\theta_{13})\cos(\delta_{\text{CP}} - \xi_2)\right] \\ & - |\Lambda_2\Lambda_3|\left[s_{12}\sin(2\theta_{13})\cos(\delta_{\text{CP}} - \xi_1)\right] ,\end{aligned}$$

Miranda, DKP, Tórtola, Valle, JHEP 1907 (2019) 103

TMMs in flavor & mass basis @ SNS facilities (delayed $\bar{\nu}_\mu$)

Delayed beam: (i) ν_e (with $\mathfrak{a}_-^1 = 1$) and (ii) $\bar{\nu}_\mu$ (with $\mathfrak{a}_+^2 = 1$)

Focus on the $\bar{\nu}_\mu$ component

- flavor basis

$$\left(\mu^F_{\bar{\nu}_\mu,\,\text{delayed}}\right)^2 = |\Lambda_e|^2 + |\Lambda_\tau|^2$$

- mass basis

$$\begin{aligned}
\left(\mu^M_{\bar{\nu}_\mu,\,\text{delayed}}\right)^2 = {} & |\Lambda_1|^2 \left[-2c_{12}c_{23}s_{12}s_{13}s_{23}\cos\delta_{CP} + s_{23}^2\left(c_{13}^2 + s_{12}^2 s_{13}^2\right) + c_{12}^2 c_{23}^2\right] \\
& + |\Lambda_2|^2 \left[2c_{12}c_{23}s_{12}s_{13}s_{23}\cos\delta_{CP} + s_{23}^2\left(c_{13}^2 + c_{12}^2 s_{13}^2\right) + s_{12}^2 c_{23}^2\right] \\
& + |\Lambda_3|^2 \left[\frac{1}{4}\left(2c_{13}^2\cos(2\theta_{23}) - \cos(2\theta_{13}) + 3\right)\right] \\
& + 2\,|\Lambda_1\Lambda_2| \left[c_{23}s_{13}s_{23}\left(c_{12}^2\cos\left(\delta_{CP} + \xi_3\right) - s_{12}^2\cos\left(\delta_{CP} - \xi_3\right)\right)\right. \\
& \left. + c_{12}c_{23}^2 s_{12}\cos\xi_3 - c_{12}s_{12}s_{13}^2 s_{23}^2\cos\xi_3\right] \\
& + 2\,|\Lambda_1\Lambda_3| \left[c_{13}s_{23}\left(c_{12}s_{13}s_{23}\cos\left(\delta_{CP} - \xi_2\right) + c_{23}s_{12}\cos\xi_2\right)\right] \\
& + 2\,|\Lambda_2\Lambda_3| \left[c_{13}s_{23}\left(s_{12}s_{13}s_{23}\cos\left(\delta_{CP} - \xi_1\right) - c_{12}c_{23}\cos\xi_1\right)\right]
\end{aligned}$$

Miranda, DKP, Tórtola, Valle, JHEP 1907 (2019) 103

Experimental configuration

Miranda, DKP, Tórtola, Valle, JHEP 1907 (2019) 103

Experiment	detector	mass	threshold	efficiency	exposure	baseline (m)
			SNS			
COHERENT	CsI[Na]	14.57 kg [100 kg]	5 keV [1 keV]	Eq. (**??**) [100%]	308.1 days [10 yr]	19.3
COHERENT	HPGe	15 kg [100 kg]	5 keV [1 keV]	50% [100%]	308.1 days [10 yr]	22
COHERENT	LAr	1 ton [10 ton]	20 keV [10 keV]	50% [100%]	308.1 days [10 yr]	29
COHERENT	NaI[Tl]	2 ton [10 ton]	13 keV [5 keV]	50% [100%]	308.1 days [10 yr]	28
			Reactor			
CONUS	Ge	3.85 kg [100 kg]	100 eV	50% [100%]	1 yr [10 yr]	17
CONNIE	Si	1 kg [100 kg]	28 eV	50% [100%]	1 yr [10 yr]	30
MINER	2Ge:1Si	1 kg [100 kg]	100 eV	50% [100%]	1 yr [10 yr]	2
TEXONO	Ge	1 kg [100 kg]	100 eV	50% [100%]	1 yr [10 yr]	28
RED100	Xe	100 kg [100 kg]	500 eV	50% [100%]	1 yr [10 yr]	19

Calculation of the number of events above threshold

$$N_{\rm theor} = \sum_{\nu_\alpha} \sum_{x={\rm isotope}} \mathcal{F}_x \int_{T_{\rm th}}^{T_A^{\rm max}} \int_{E_\nu^{\rm min}}^{E_\nu^{\rm max}} f_{\nu_\alpha}(E_\nu) \mathcal{A}(T_A) \left(\frac{d\sigma_x}{dT_A}(E_\nu, T_A) \right)_{\rm tot} dE_\nu dT_A \,,$$

- luminosity for a detector with target material x: $\mathcal{F}_x = N^x_{\rm targ} \Phi_\nu$
- $E_\nu^{\rm min} = \sqrt{m_A T_A/2}$: the minimum incident neutrino energy to produce a nuclear recoil

Statistical analysis

First phase of COHERENT (with a CsI detector)

$$\chi^2(\mathcal{S}) = \min_{a_1, a_2} \left[\frac{(N_{\rm meas} - N_{\rm theor}(\mathcal{S})[1+a_1] - B_{0n}[1+a_2])^2}{(\sigma_{\rm stat})^2} + \left(\frac{a_1}{\sigma_{a_1}}\right)^2 + \left(\frac{a_2}{\sigma_{a_2}}\right)^2 \right].$$

- measured number of events is $N_{\rm meas} = 142$,
- a_1 and a_2 are the systematic uncertainties (signal and background rates), with $\sigma_{a_1} = 0.28$ and $\sigma_{a_2} = 0.25$.
- Statistical uncertainty $\sigma_{\rm stat} = \sqrt{N_{\rm meas} + B_{0n} + 2B_{ss}}$, where the quantities $B_{0n} = 6$ and $B_{ss} = 405$ denote the beam-on prompt neutron and the steady-state background events respectively.

Reactor experiments and next generation of COHERENT

$$\chi^2(\mathcal{S}) = \min_{a} \left[\frac{(N_{\rm meas} - N_{\rm theor}(\mathcal{S})[1+a])^2}{(1+\sigma_{\rm stat})N_{\rm meas}} + \left(\frac{a}{\sigma_{\rm sys}}\right)^2 \right],$$

- with $\sigma_{stat} = \sigma_{\rm sys} = 0.2$ (0.1) for the current (future) setups.

Probe TMMs through minimization over the nuisance parameter a and calculate $\Delta\chi^2(\mathcal{S}) = \chi^2(\mathcal{S}) - \chi^2_{\rm min}(\mathcal{S})$, with $\mathcal{S} \equiv \{|\Lambda_i|, \xi_i, \delta_{\rm CP}\}$

Analysis of CEνNS data: sensitivity to $|\Lambda_i|$

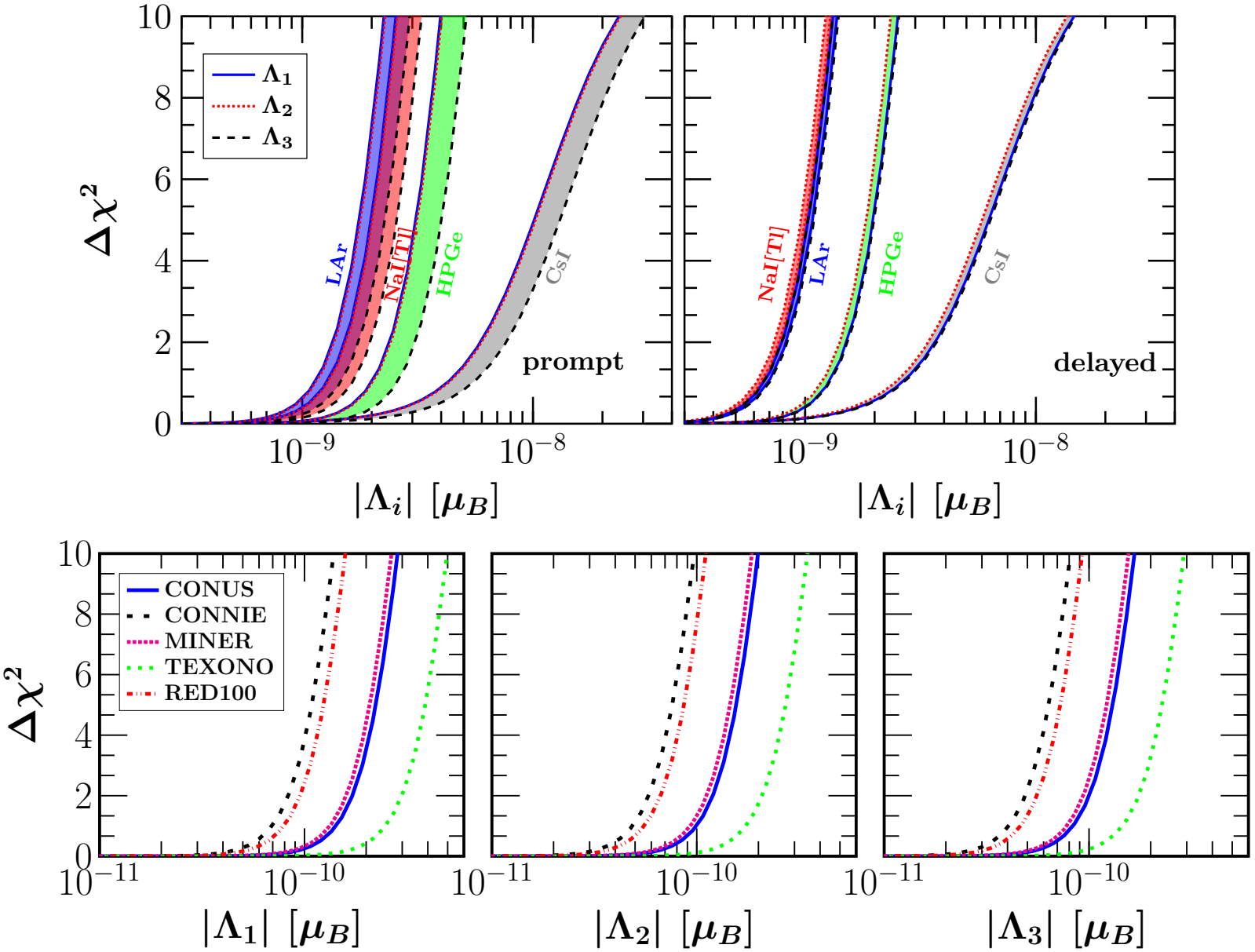

all results in units $10^{-10}\mu_B$

Miranda, DKP, Tórtola, Valle, JHEP 1907 (2019) 103

Estimating the future prospects: luminosity factor variation

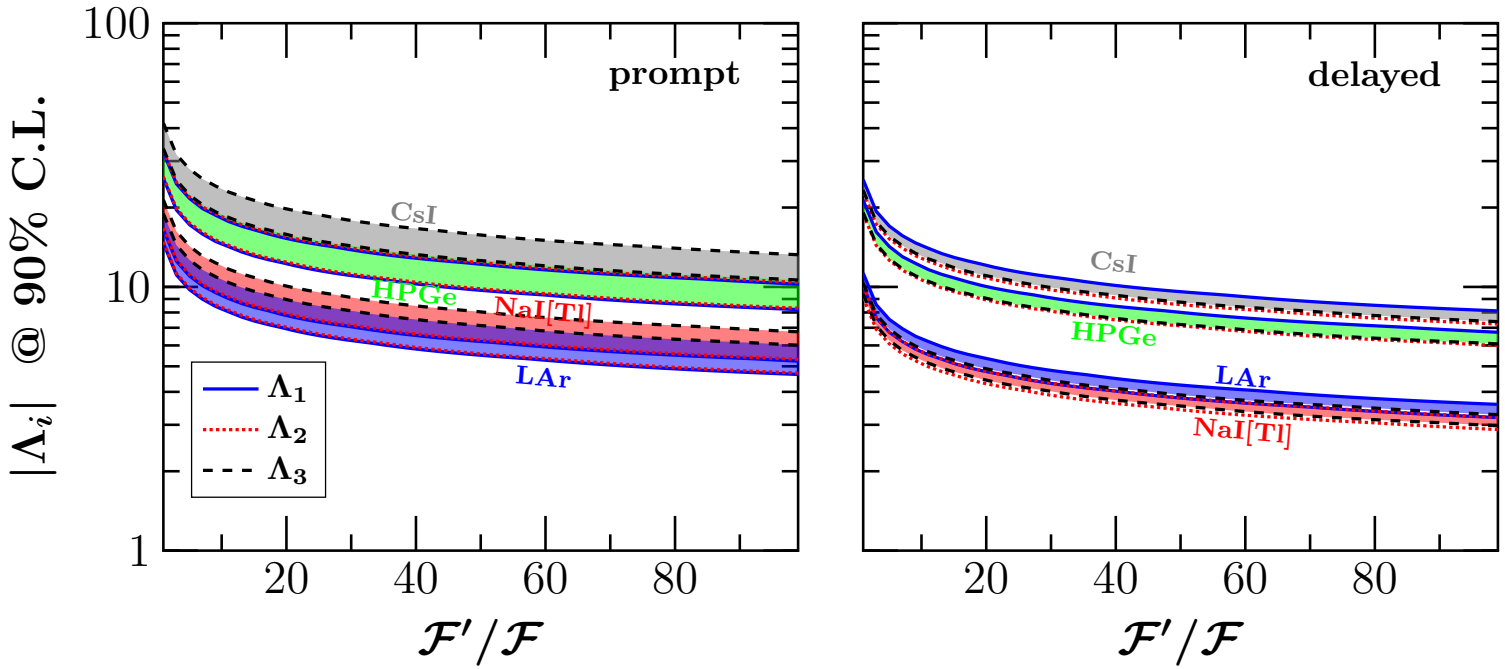

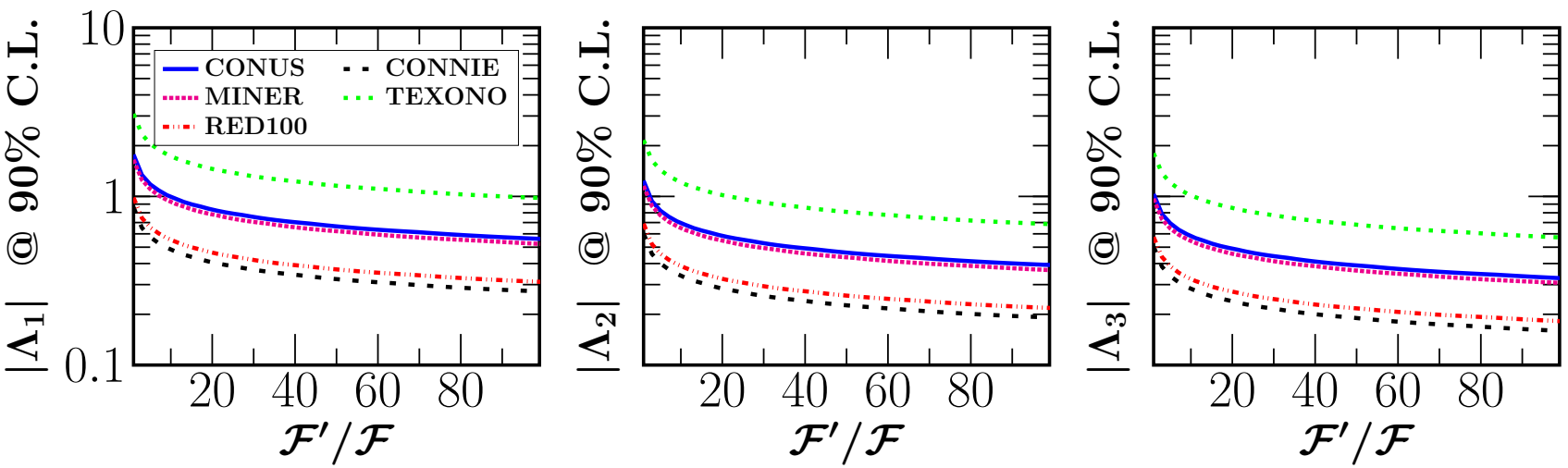

all results in units $10^{-10}\mu_B$

Miranda, DKP, Tórtola, Valle, JHEP 1907 (2019) 103

Current COHERENT setup: combined constraints

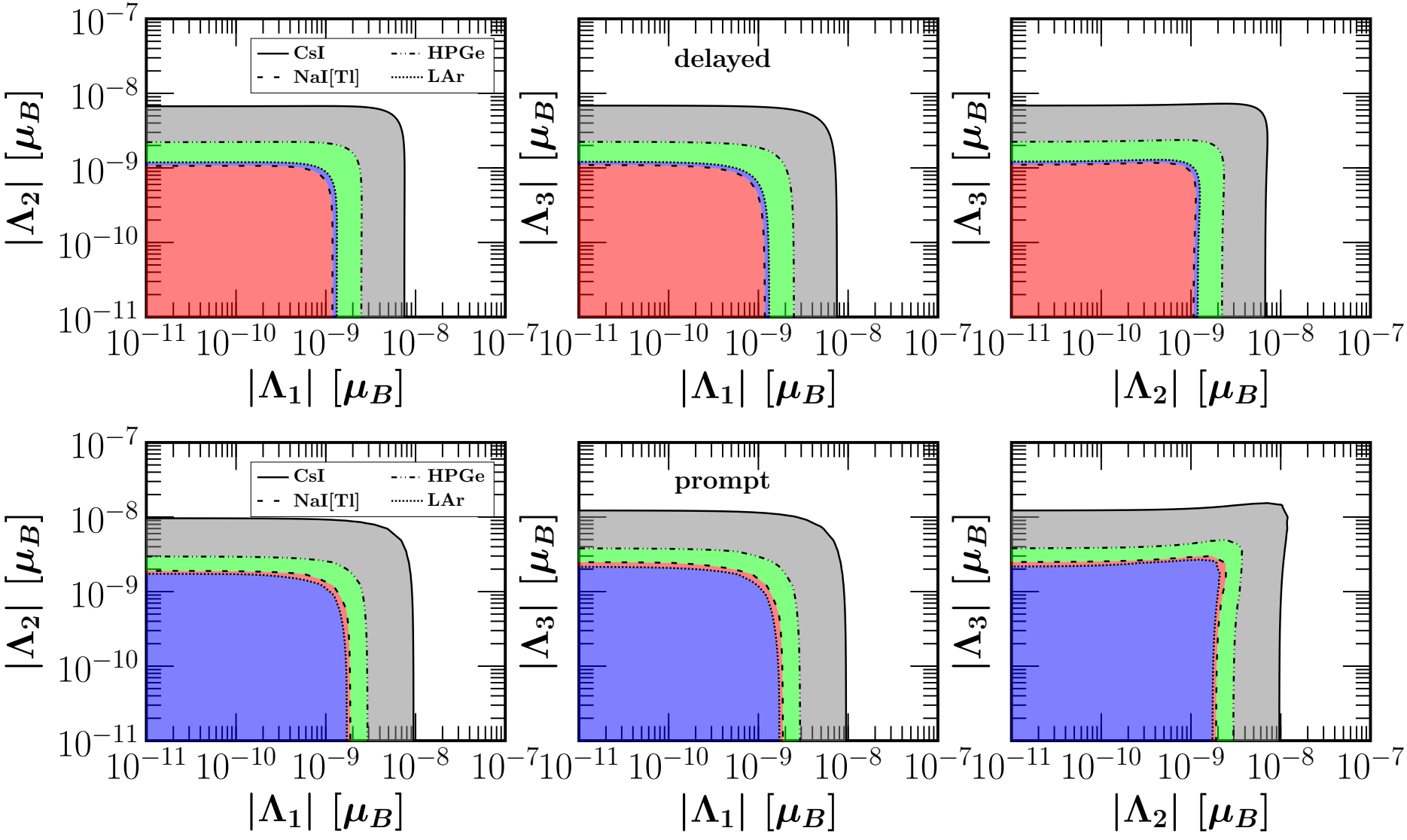

Miranda, DKP, Tórtola, Valle, JHEP 1907 (2019) 103

Future COHERENT setup: combined constraints

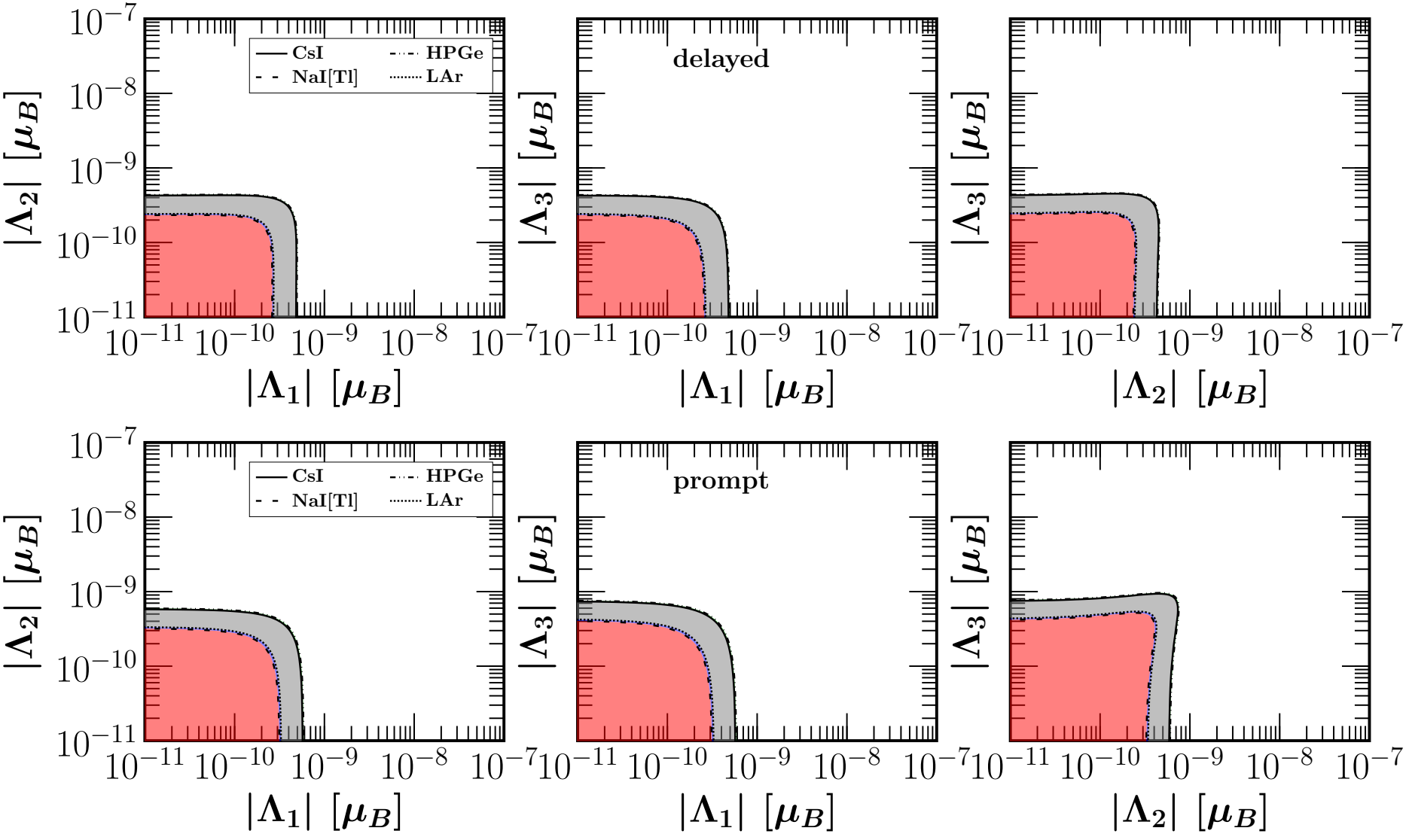

Miranda, DKP, Tórtola, Valle, JHEP 1907 (2019) 103

Current & Future Reactor experiments: combined constraints

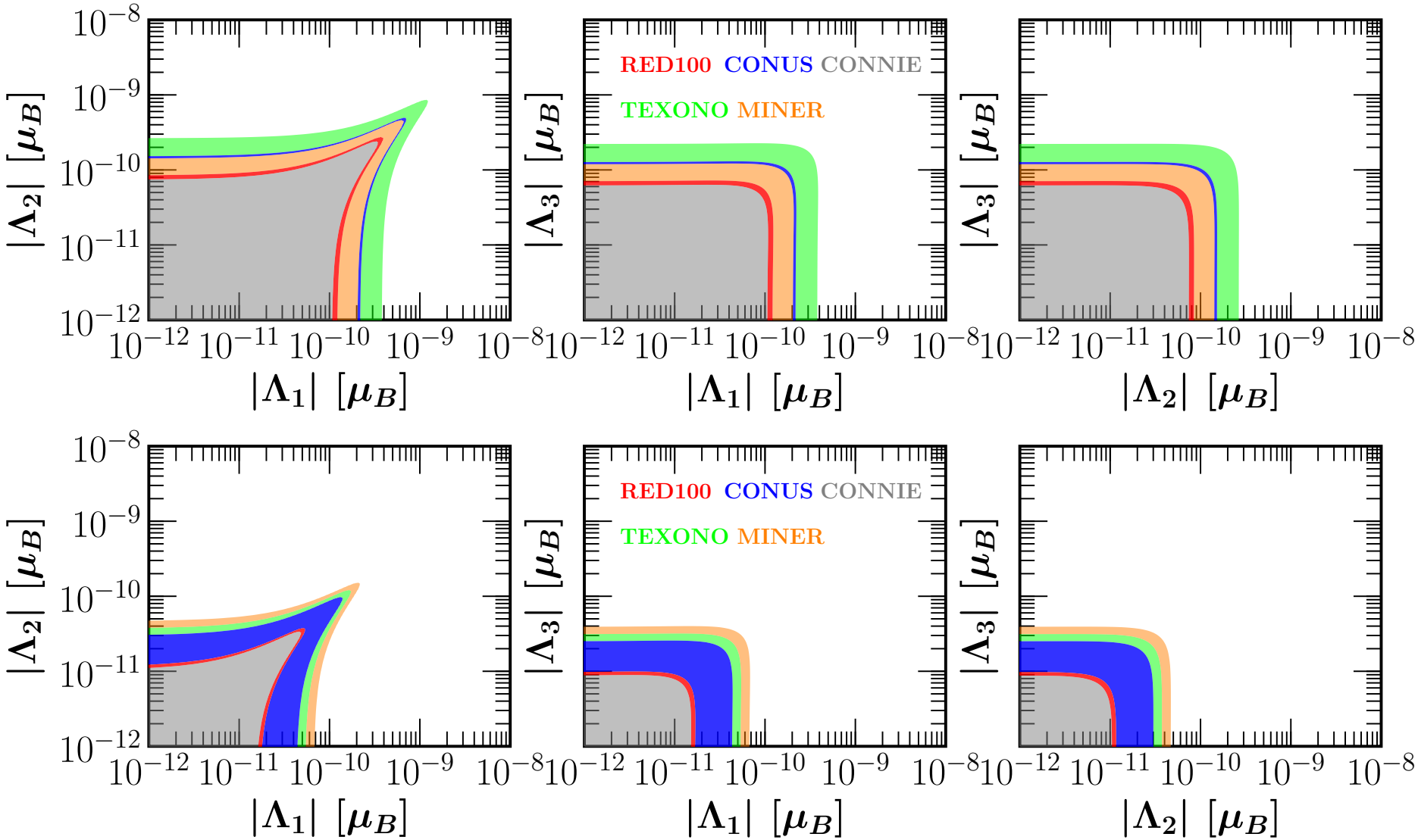

Miranda, DKP, Tórtola, Valle, JHEP 1907 (2019) 103

Solar neutrinos from Borexino

Miranda, DKP, Tórtola, Valle, JHEP 1907 (2019) 103

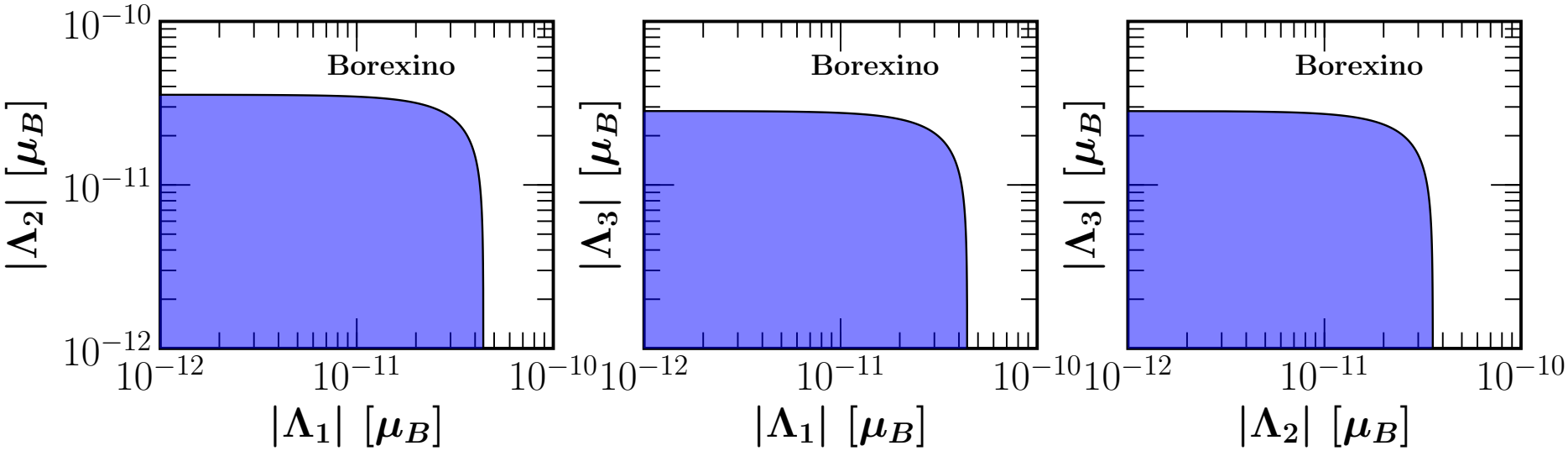

- solar electron neutrinos undergo flavor oscillations arriving to the detector as an incoherent admixture of mass eigenstates (no phase dependence)
- dependence on neutrino mixing and oscillation factor between the source and detection is considered $\left(\mu^M_{\nu,\text{eff}}\right)^2(L,E_\nu) = \sum_j \left|\sum_i U^*_{\alpha i} e^{-i\,\Delta m^2_{ij} L/2E_\nu}\,\tilde{\lambda}_{ij}\right|^2$
- the oscillation probabilities from ν_e to mass eigenstates ν_i are approximated

$$P^{3\nu}_{e3} = \sin^2\theta_{13}, \quad P^{3\nu}_{e1} = \cos^2\theta_{13} P^{2\nu}_{e1}, \quad P^{3\nu}_{e2} = \cos^2\theta_{13} P^{2\nu}_{e2},$$

  and the unitarity condition, $P^{2\nu}_{e1} + P^{2\nu}_{e2} = 1$
- effective neutrino magnetic moment for solar neutrinos in mass basis [Cañas et al.: PLB 753 (2016)]

$$(\mu^M_{\nu,\,\text{sol}})^2 = |\mathbf{\Lambda}|^2 - c^2_{13}|\Lambda_2|^2 + (c^2_{13}-1)|\Lambda_3|^2 + c^2_{13} P^{2\nu}_{e1}(|\Lambda_2|^2 - |\Lambda_1|^2)$$

- Recall Borexino phase-II limit $\mu_\nu < 2.8\times 10^{-11}\mu_B$ [Borexino Collab., Agostini et al.:PRD 96 (2017)]

Impact of CP phases

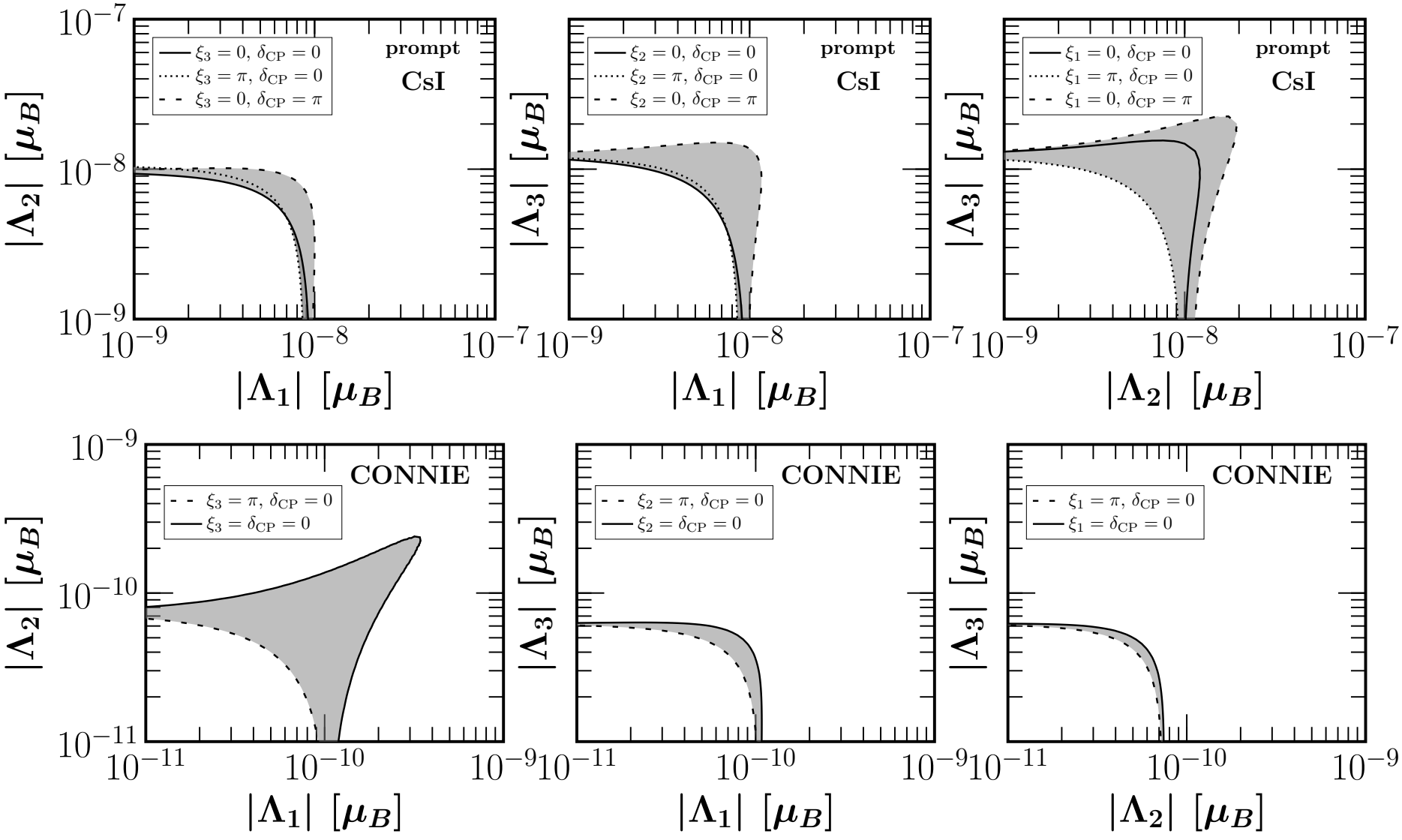

explore the robustness of TMMs limits

Miranda, DKP, Tórtola, Valle, JHEP 1907 (2019) 103

Constraints on TMMs from CEvNS experiments

Experiment	$\lvert\Lambda_1\rvert$	$\lvert\Lambda_2\rvert$	$\lvert\Lambda_3\rvert$
	SNS prompt		
CsI[Na]	69.2 [5.0]	70.2 [5.1]	89.6 [6.4]
HPGe	25.9 [5.1]	26.2 [5.2]	33.5 [6.6]
LAr	14.7 [2.9]	14.9 [2.9]	19.1 [3.7]
NaI[Tl]	16.6 [2.8]	16.8 [2.8]	21.5 [3.6]
	SNS delayed		
CsI[Na]	54.5 [4.2]	48.7 [3.7]	49.8 [3.7]
HPGe	21.3 [4.2]	18.9 [3.8]	19.1 [3.8]
LAr	11.3 [2.3]	10.1 [2.1]	10.4 [2.1]
NaI[Tl]	10.0 [2.3]	9.1 [2.0]	9.4 [2.0]
	Reactor		
CONUS	1.9 [0.37]	1.3 [0.26]	1.1 [0.22]
CONNIE	0.90 [0.13]	0.63 [0.09]	0.53 [0.08]
MINER	1.7 [0.58]	1.2 [0.41]	1.0 [0.34]
TEXONO	3.2 [0.46]	2.3 [0.32]	1.9 [0.27]
RED100	1.0 [0.14]	0.72 [0.10]	0.61 [0.08]
	Solar		
Borexino	0.44	0.36	0.28

90% C.L. limits on TMM elements $|\Lambda_i|$, in units of 10^{-10} μ_B, from current and future CEνNS experiments. The numbers in square brackets indicate the attainable sensitivities in the future setups.

- CEνNS experiments are sensitive to EM neutrino properties
- can probe TMMs at $10^{-11}\mu_B$ at least
- competitive with large-scale solar neutrino experiments

Miranda, DKP, Tórtola, Valle, JHEP 1907 (2019) 103

Analysis of the COHERENT data: SM

- **SM diff. cross section**

$$\frac{d\sigma_{\rm SM}}{dT_N}(E_\nu, T_N) = \frac{G_F^2 M}{\pi}\left[(\mathcal{Q}_W^V)^2\left(1-\frac{MT_N}{2E_\nu^2}\right) + (\mathcal{Q}_W^A)^2\left(1+\frac{MT_N}{2E_\nu^2}\right)\right]F^2(T_N)\,,$$

- **SM vector and axial vector couplings**

$$\mathcal{Q}_W^V = \left[g_p^V Z + g_n^V N\right]\,,$$
$$\mathcal{Q}_W^A = \left[g_p^A(Z_+ - Z_-) + g_n^A(N_+ - N_-)\right]\,,$$

- **single-bin counting problem (flux, quenching factor, and acceptance uncertainties are incorporated)**

$$\chi^2(s_W^2) = \min_{\xi,\zeta}\left[\frac{\left(N_{\rm meas} - N_{\nu_\alpha}^{\rm SM}(s_W^2)[1+\xi] - B_{0n}[1+\zeta]\right)^2}{\sigma_{\rm stat}^2} + \left(\frac{\xi}{\sigma_\xi}\right)^2 + \left(\frac{\zeta}{\sigma_\zeta}\right)^2\right],$$

DKP and T.S. Kosmas, Phys.Rev. **D97** (2018) 033003

for future perspectives see Cañas et al., Phys.Lett. B784 (2018) 159-162

- **search between $6 \leq n_{\rm PE} \leq 30$**

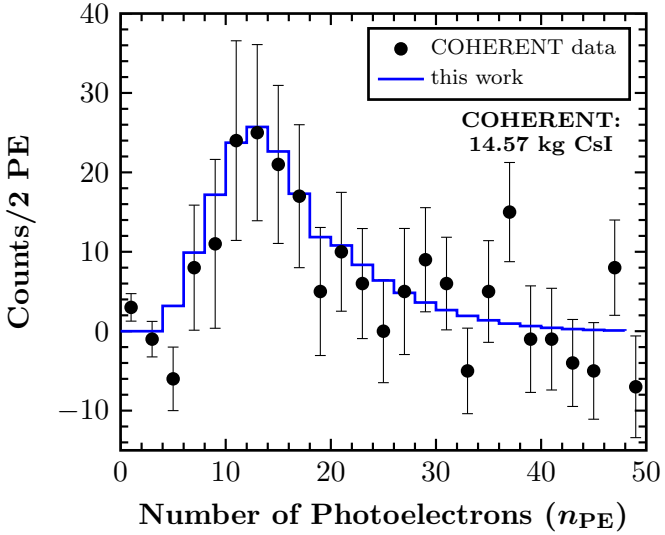

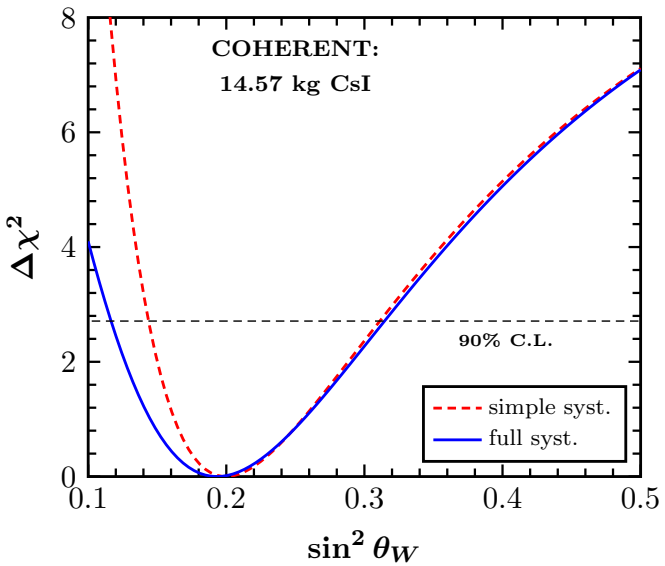

Analysis of the COHERENT data: EM properties

- **Neutrino magnetic moment contrbution**

$$\left(\frac{d\sigma}{dT_N}\right)_{\rm SM+EM} = \mathcal{G}_{\rm EM}(E_\nu, T_N)\frac{d\sigma_{\rm SM}}{dT_N} ,$$

$$\mathcal{G}_{\rm EM} = 1 + \frac{1}{G_F^2 M}\left(\frac{\mathcal{Q}_{\rm EM}}{\mathcal{Q}_W^V}\right)^2 \frac{\frac{1-T_N/E_\nu}{T_N}}{1-\frac{MT_N}{2E_\nu^2}} .$$

- **EM charge:** $\mathcal{Q}_{\rm EM} = \frac{\pi a_{\rm EM}\mu_{\nu_\alpha}}{m_e} Z$
  Vogel et al. Phys.Rev. D39 (1989) 3378

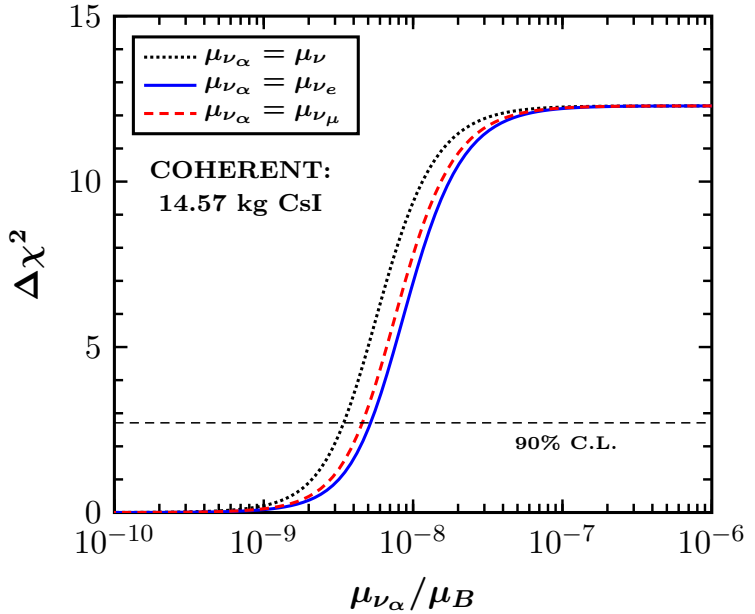

- **Neutrino charge radius**
- **redefinition of the weak mixing angle**

$$\sin^2\theta_W \to \sin^2\overline{\theta_W} + \frac{\sqrt{2}\pi a_{\rm EM}}{3G_F}\langle r^2_{\nu_\alpha}\rangle .$$

see also Cadeddu et al., arXiv:1810.05606

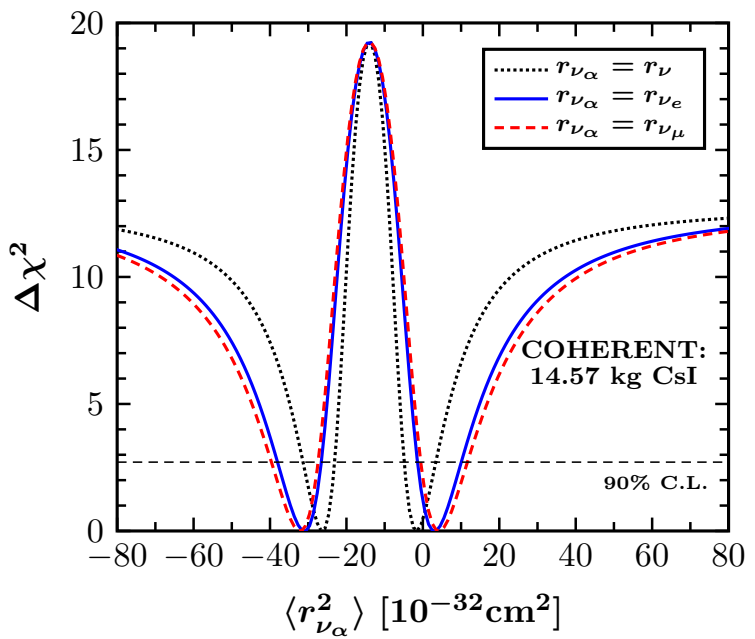

DKP and T.S. Kosmas, Phys.Rev. **D97** (2018) 033003

Analysis of the COHERENT data: combined constraints

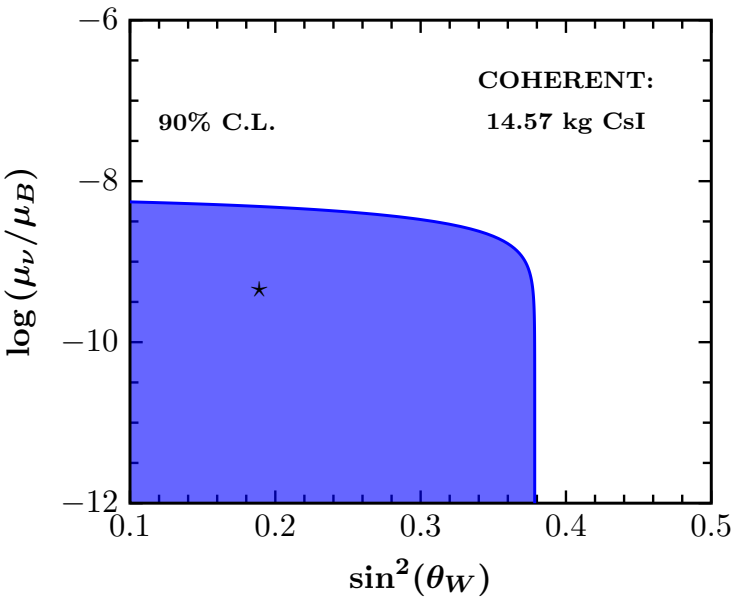

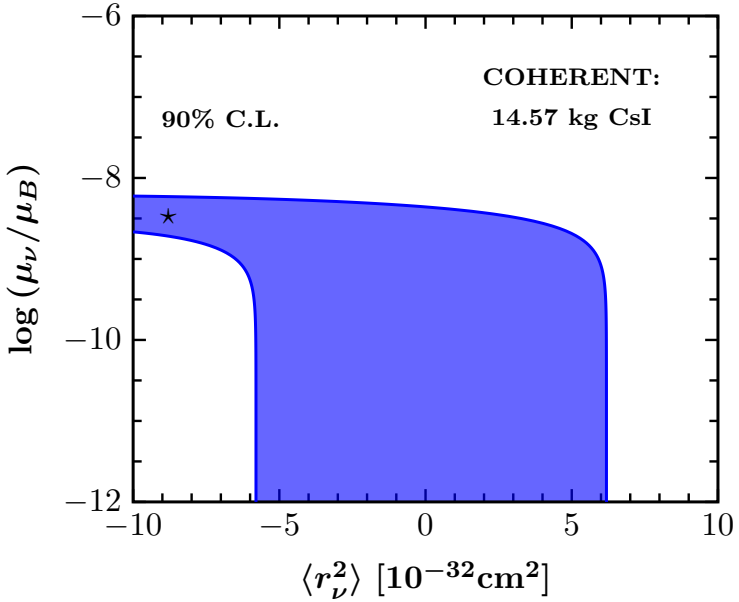

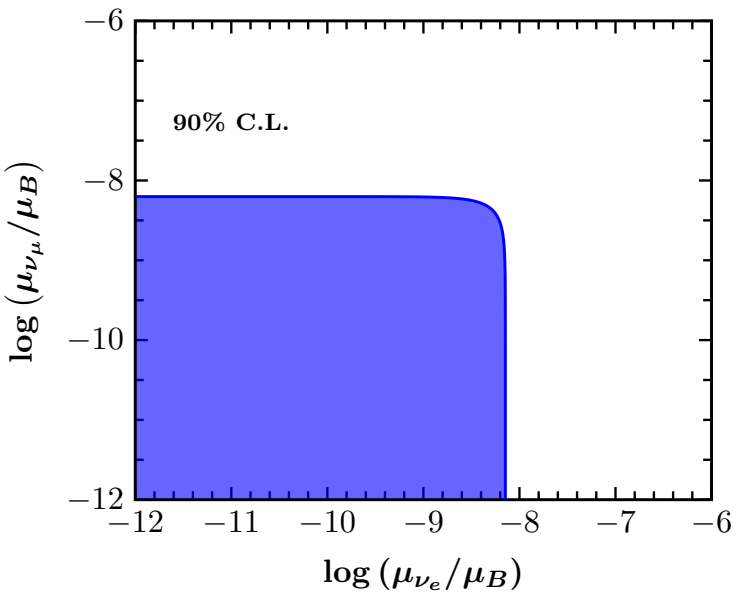

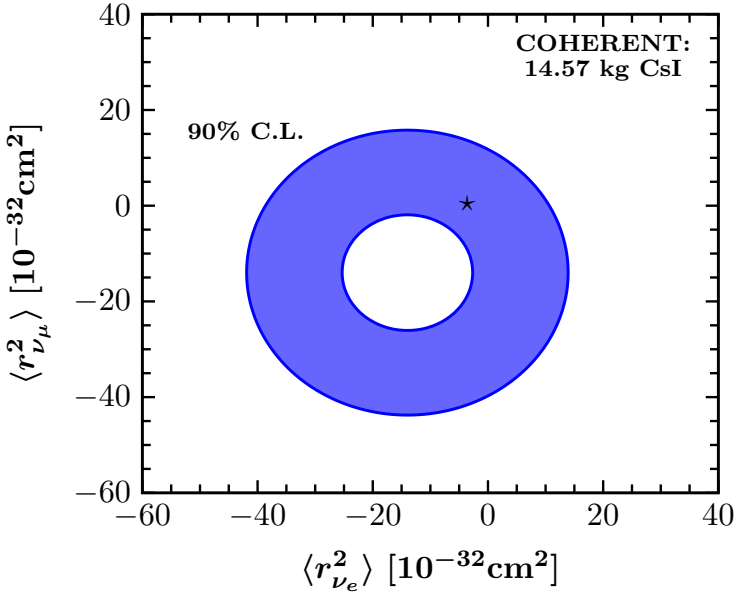

DKP and T.S. Kosmas, Phys.Rev. **D97** (2018) 033003

Probing the neutron radii: nuclear form factor

COHERENT	$\mathcal{F}'/\mathcal{F}$	stat. uncertainty	syst. uncertainty	$b\,(\mathrm{fm}^{-1})$	$\langle R_n^2\rangle^{1/2}$ (fm)
phase I	1	current	current	$2.30^{+0.36}_{-0.54}$	$5.64^{+0.99}_{-1.2}$
scenario I	10	$\sigma_{\mathrm{stat}} = 0.2$	$\sigma_{\mathrm{sys}} = 0.14$	$2.10^{+0.16}_{-0.21}$	$5.56^{+0.97}_{-0.49}$
scenario II	100	$\sigma_{\mathrm{stat}} = 0.1$	$\sigma_{\mathrm{sys}} = 0.07$	$2.10^{+0.08}_{-0.08}$	$5.56^{+0.19}_{-0.23}$

Model independent form factor expansion Patton et al. Phys.Rev. C86 (2012)

$$F_{p,n}(Q^2) \approx 1 - \frac{Q^2}{3!}\langle R^2_{p,n}\rangle + \frac{Q^4}{5!}\langle R^4_{p,n}\rangle - \frac{Q^6}{7!}\langle R^6_{p,n}\rangle + \cdots ,$$

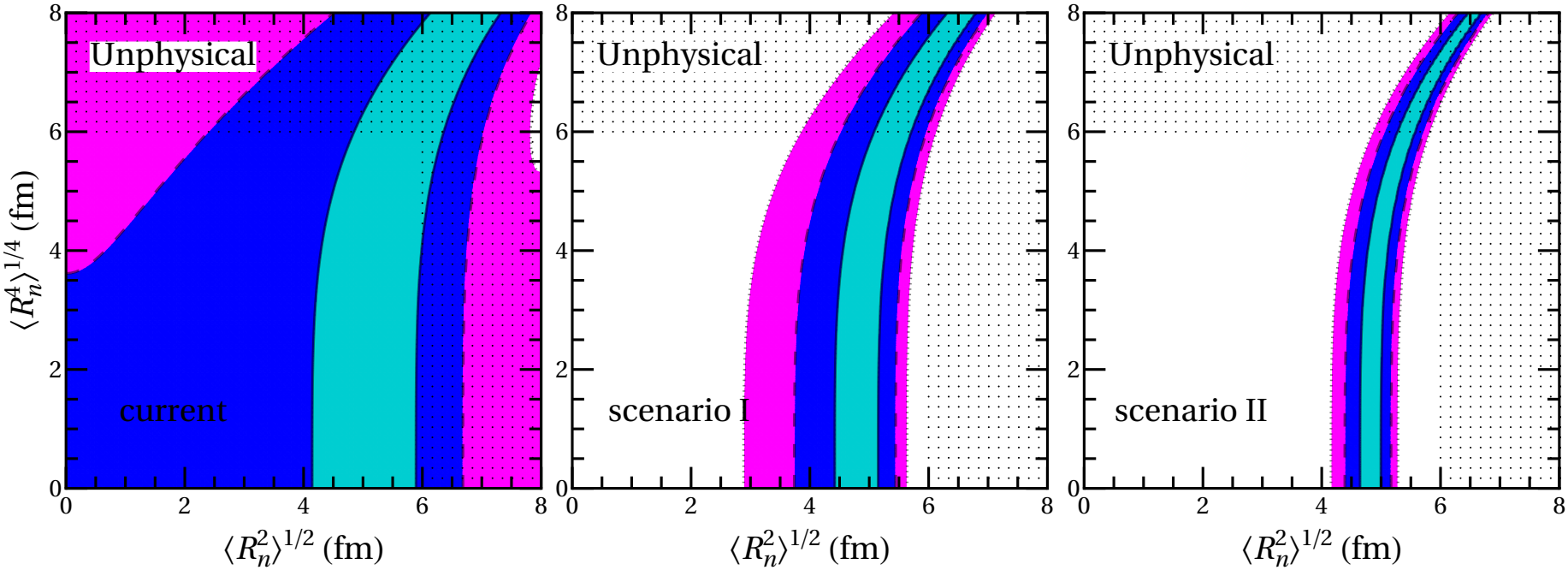

DKP et al. arXiv:1903.03722

Probing nuclear physics

Follows from the convolution of a Yukawa potential with range $a_k = 0.7$ fm over a Woods-Saxon distribution, approximated as a hard sphere with radius R_A.

$$F_{\rm KN} = 3\frac{j_1(QR_A)}{qR_A}\left[1+(Qa_k)^2\right]^{-1}$$

The rms radius is: $\langle R^2\rangle_{\rm KN} = 3/5R_A^2 + 6a_k^2$

S. Klein and J. Nystrand, Phys.Rev. C60 (1999) 014903

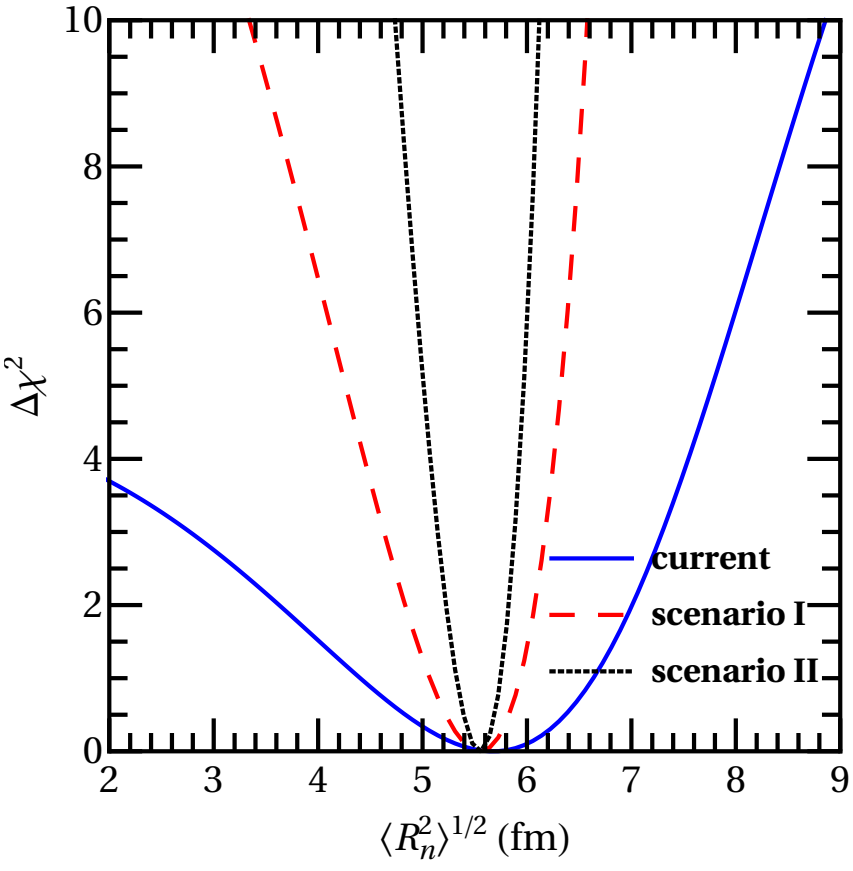

DKP et al. arXiv:1903.03722

Summary

SM CEνNS reaction (conventional)

$$\nu_\alpha + (A, Z) \to \nu_\alpha + (A, Z), \quad \alpha = (e, \mu, \tau)$$

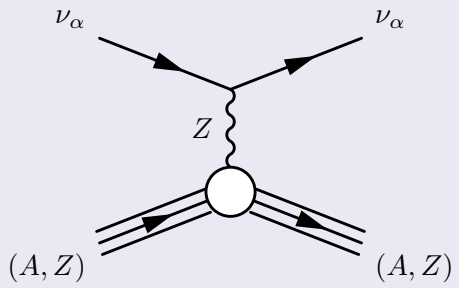

- Conventional, well-studied ν-process theoretically
- Finally observed by COHERENT in August 2017, CONUS (hints)
  (other: MINER, TEXONO, CONNIE, Ricochet, νGEN, ν-cleus etc.)
- Very high experimental sensitivity (low detector threshold) is required

- presented the effective μ_ν formalism in terms of fundamental parameters relevant to terrestrial neutrino experiments
- current and future limits on $|\Lambda_i|$ from low-energy CEνNS experiments (of the order of $10^{-11}\mu_B$ at least)
- demonstrated that CEνNS experiments can be competitive to large-scale ones e.g. with Borexino
- obtained constraints on the neutrino charge radii
- determined the weak-mixing angle $\sin^2\theta_W$ at low-energy
- explored the neutron rms radius

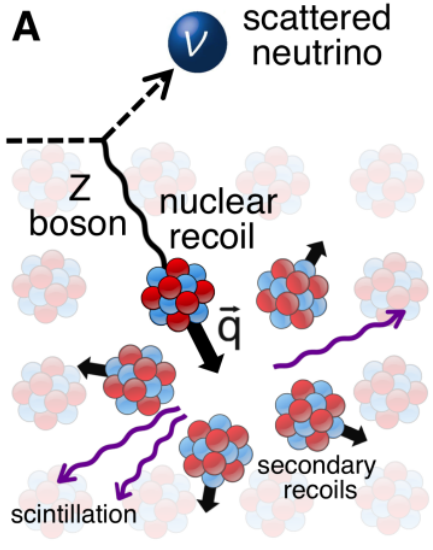

Thank you for your attention !

Extras

SM Cross sections and Nuclear Transition Matrix Elements

The SM CEνNS diff. cross section with respect to the nuclear recoil energy T_N takes the form

$$\frac{d\sigma_{\mathrm{SM},\nu_\alpha}}{dT_N} = \frac{G_F^2}{\pi}\left(1 - \frac{MT_N}{2E_\nu^2}\right)\left|\langle g.s.||\mathcal{M}^{\mathrm{SM}}_{V,\nu_\alpha}||g.s.\rangle\right|^2$$

- E_ν: incident neutrino energy
- $q^2 = -MT_N$: 4-momentum transfer (from kinematics: $-q^2 \equiv Q^2 = -\omega^2 + \mathbf{q}^2 > 0$)
- $|g.s.\rangle = |J^\pi\rangle \equiv |0^+\rangle$: the nuclear ground state
  (for even-even nuclei is explicitly constructed by solving the BCS Eqs.)
- $g_V^{p(n)}$: polar-vector coupling of proton (neutron) to the Z boson

- The SM nuclear matrix element is given in terms of the electromagnetic proton(neutron) nuclear form factors $F_{Z(N)}(Q^2)$ (CVC theory)
- For SM $g.s. \to g.s.$ transitions (i.e. $|0^+\rangle \to |0^+\rangle$) only the Coulomb operator contributes

$$\left|\mathcal{M}^{\mathrm{SM}}_{V,\nu_\alpha}\right|^2 \equiv \left|\langle g.s.||\hat{\mathcal{M}}_{00}||g.s.\rangle\right|^2 = \left[g_V^p Z F_Z(Q^2) + g_V^n N F_N(Q^2)\right]^2$$

DKP and T.S. Kosmas, Phys.Lett. **B728** (2014) 482

Incoherent neutrino-nucleus scattering

- Interaction Hamiltonian for neutral-current (NC) neutrino-nucleus scattering

$$\langle f|\hat{H}_{eff}|i\rangle = \frac{G_F}{\sqrt{2}}\int d^3\mathbf{x}\,\langle \ell_f|\hat{j}^{lept}_{\mu}(\mathbf{x})|\ell_i\rangle\langle J_f|\hat{\mathcal{J}}^{\mu}(\mathbf{x})|J_i\rangle$$

with $\langle \ell_f|\hat{j}^{lept}_{\mu}|\ell_i\rangle = \bar{\nu}_\alpha\gamma_\mu(1-\gamma_5)\nu_\alpha\, e^{-i\mathbf{q}\cdot\mathbf{x}}$, $\quad \mathbf{q}: 3-\text{momentum transfer}$

- In the Donnelly-Walecka multipole decomposition method, the NC, double diff. SM cross section from an initial $|J_i\rangle$ to a final $|J_f\rangle$ nuclear state (constructed explicitly through QRPA realistic nuclear structure calculations), reads

$$\boxed{\frac{d^2\sigma_{i\to f}}{d\Omega\, d\omega} = \frac{G_F^2}{\pi}\frac{\varepsilon_i\varepsilon_f}{(2J_i+1)}\left(\sum_{J=0}^{\infty}\sigma^J_{\rm CL}+\sum_{J=1}^{\infty}\sigma^J_{\rm T}\right),}$$

ε_i (ε_f) is the initial (final) neutrino energy and ω is the nucleus excitation energy.

- Contributions to $\sigma^J_{\rm CL}$ (Coulomb-longitudinal) and $\sigma^J_{\rm T}$ (transverse electric-magnetic) components T. W. Donnelly and R. D. Peccei, Phys. Rept. **50** (1979) 1

$$\begin{aligned}
\sigma^J_{\rm CL} =&(1+a\cos\theta)|\langle J_f||\hat{\mathcal{M}}_J(\kappa)||J_i\rangle|^2+(1+a\cos\theta-2b\sin^2\theta)|\langle J_f||\hat{\mathcal{L}}_J(\kappa)||J_i\rangle|^2\\
&+\left[\frac{\omega}{\kappa}(1+a\cos\theta)+d\right]2\Re e|\langle J_f||\hat{\mathcal{L}}_J(\kappa)||J_i\rangle||\langle J_f||\hat{\mathcal{M}}_J(\kappa)||J_i\rangle|^*,\\
\sigma^J_{\rm T} =&(1-a\cos\theta+b\sin^2\theta)\left[|\langle J_f||\hat{\mathcal{T}}^{mag}_J(\kappa)||J_i\rangle|^2+|\langle J_f||\hat{\mathcal{T}}^{el}_J(\kappa)||J_i\rangle|^2\right]\\
&\mp\left[\frac{(\varepsilon_i+\varepsilon_f)}{\kappa}(1-a\cos\theta)-d\right]2\Re e|\langle J_f||\hat{\mathcal{T}}^{mag}_J(\kappa)||J_i\rangle||\langle J_f||\hat{\mathcal{T}}^{el}_J(\kappa)||J_i\rangle|^*
\end{aligned}$$

where the parameters $a=1$, $b=\varepsilon_i\varepsilon_f/\kappa^2$, $d=0$ are obtained from the kinematics and $\kappa=|\mathbf{q}|$

Evaluation of the Nuclear Matrix Elements

- Seven new operators are defined (proton-neutron representation) as

$$
\begin{aligned}
T_1^{JM} &\equiv M_M^J(\kappa \mathbf{r}) = \delta_{LJ}\, j_L(\kappa r) Y_M^L(\hat{r}), \\
T_2^{JM} &\equiv \Sigma_M^J(\kappa \mathbf{r}) = \mathbf{M}_M^{JJ} \cdot \boldsymbol{\sigma}, \\
T_3^{JM} &\equiv \Sigma'^J_M(\kappa \mathbf{r}) = -i \left[\frac{1}{\kappa} \boldsymbol{\nabla} \times \mathbf{M}_M^{JJ}(\kappa \mathbf{r}) \right] \cdot \boldsymbol{\sigma}, \\
T_4^{JM} &\equiv \Sigma''^J_M(\kappa \mathbf{r}) = \left[\frac{1}{\kappa} \boldsymbol{\nabla} M_M^J(\kappa \mathbf{r}) \right] \cdot \boldsymbol{\sigma}, \\
T_5^{JM} &\equiv \Delta_M^J(\kappa \mathbf{r}) = \mathbf{M}_M^{JJ}(\kappa \mathbf{r}) \cdot \frac{1}{\kappa} \boldsymbol{\nabla}, \\
T_6^{JM} &\equiv \Delta'^J_M(\kappa \mathbf{r}) = -i \left[\frac{1}{\kappa} \boldsymbol{\nabla} \times \mathbf{M}_M^{JJ}(\kappa \mathbf{r}) \right] \cdot \frac{1}{\kappa} \boldsymbol{\nabla}, \\
T_7^{JM} &\equiv \Omega_M^J(\kappa \mathbf{r}) = M_M^J(\kappa \mathbf{r}) \boldsymbol{\sigma} \cdot \frac{1}{\kappa} \boldsymbol{\nabla}\,.
\end{aligned}
$$

Closed compact analytic formulae for the single-particle reduced ME (upper) and many-body reduced ME (lower) for QRPA calculations, are deduced.

$$
\langle (n_1 \ell_1) j_1 || T_i^J || (n_2 \ell_2) j_2 \rangle = e^{-y} y^{\beta/2} \sum_{\mu=0}^{n_{max}} \mathcal{P}_\mu^{i,J} y^\mu, \quad y = (\kappa b/2)^2, \quad n_{max} = (N_1 + N_2 - \beta)/2, \quad N_i = 2n_i + \ell_i
$$

$$
\langle f \| \widehat{T}^J \| 0^+_{gs} \rangle = \sum_{j_2 \geq j_1} \frac{\langle j_2 \| \widehat{T}^J \| j_1 \rangle}{\hat{J}} \left[X_{j_2 j_1} u_{j_2}^{p(n)} v_{j_1}^{p(n)} + Y_{j_2 j_1} v_{j_2}^{p(n)} u_{j_1}^{p(n)} \right]
$$

V.Ch. Chasioti and T.S. Kosmas, Nucl. Phys. **A 829** (2009) 234
P.G. Giannaka, DKP, T.S. Kosmas, unpublished (for any configuration $(j_1, j_2)J$)

Evaluation of the form factors (Helm)

Convolution of two nucleonic densities, one being a uniform density with cut-off radius R_0, (namely box or diffraction radius) characterizing the interior density and a second one that is associated with a Gaussian falloff in terms of the surface thickness s.

$$F_{\text{Helm}}(Q^2) = F_B F_G = 3\frac{j_1(QR_0)}{qR_0}\, e^{-(Qs)^2/2}$$

The first three moments

$$\begin{aligned}
\langle R_n^2 \rangle &= \frac{3}{5}R_0^2 + 3s^2 \\
\langle R_n^4 \rangle &= \frac{3}{7}R_0^4 + 6R_0^2 s^2 + 15s^4 \\
\langle R_n^6 \rangle &= \frac{1}{3}R_0^6 + 9R_0^4 s^2 + 63R_0^2 s^4 + 105s^6 \,.
\end{aligned}$$

- $j_1(x)$ is the known first-order Spherical-Bessel function
- box or diffraction radius R_0 (interior density)
- $s = 0.9$ fm: surface thickness of the nucleus from spectroscopy data (Gaussian fallof).

J. Engel, Phys.Lett. **B 264** (1991) 114

Evaluation of the form factors (Symmetrized Fermi)

Adopting a conventional Fermi (Woods-Saxon) charge density distribution, the SF form factor is written in terms of two parameters (c, a)

$$F_{\mathrm{SF}}\left(Q^2\right) = \frac{3}{Qc\left[(Qc)^2 + (\pi Qa)^2\right]}\left[\frac{\pi Qa}{\sinh(\pi Qa)}\right]\left[\frac{\pi Qa\sin(Qc)}{\tanh(\pi Qa)} - Qc\cos(Qc)\right],$$

The first three moments

$$\begin{aligned}
\left\langle R_n^2\right\rangle &= \frac{3}{5}c^2 + \frac{7}{5}(\pi a)^2 \\
\left\langle R_n^4\right\rangle &= \frac{3}{7}c^4 + \frac{18}{7}(\pi a)^2c^2 + \frac{31}{7}(\pi a)^4 \\
\left\langle R_n^6\right\rangle &= \frac{1}{3}c^6 + \frac{11}{3}(\pi a)^2c^4 + \frac{239}{15}(\pi a)^4c^2 + \frac{127}{5}(\pi a)^6 .
\end{aligned}$$

- c: half-density radius
- a fm: diffuseness
- surface thickness: $t = 4a\ln 3$

J.D. Lewin and P.F. Smith, Astropart.Phys. 6 (1996) 87-112